Drying of Solids in a Rotary Dryer

HLQ Induction Equipment Co.,Ltd

https://dw-inductionheater.com

Experiments were conducted in a batch rotary dryer for obtaining the drying kinetics of a non-hygroscopic material with preheated air as the drying medium. The progress of the drying process was investigated for different temperatures and flow rates of the drying medium, initial moisture content of the solids, and rotational speed of the dryer. The contacting pattern of the same dryer was obtained through Residence Time Distribution (RTD) studies and the variables include rotational speed and inclination of the dryer and feed rate of the solids. The RTD data was subjected to axial dispersion model and axial dispersion number was estimated. Correlations were proposed for mean residence time, hold-up of the solids, and dispersion number. The performance of the continuous dryer was predicted through batch kinetics and RTD, and the predictions were validated with experimental data. The study shows that the drying kinetics coupled with residence time distribution function for the flow of the solids satisfactorily predicts the moisture content of the solids in the product in a continuous dryer.

Keywords Continuous drying; Drying kinetics; Rotary dryer; RTD

INTRODUCTION

Drying is an operation of great commercial importance in many industrial applications ranging through the food, agricultural, mining, and manufacturing sectors. Drying is certainly one of the most energy-intensive operations in industry and most dryers operate at low thermal efficiency. Drying is a process in which an unbound and/or bound volatile liquid is removed from a solid by evaporation. Large quantities of granular material with particles of 10 mm or larger that are not too fragile or heat-sensitive, or cause any other handling problems are dried in rotary dryers in process industries.

The conventional heat transfer methods for drying are convection, conduction, and infrared radiation and dielectric heating. In modern drying techniques, internal heat is generated by radio or microwave frequencies. In most dryers heat is transferred by more than one method, but each industrial dryer has one predominant heat transfer method. In the rotary dryer this is convection, the necessary heat usually being provided by direct contact of a hot gas with the wet solid. Rotary drying is a complicated process involving simultaneous heat, mass transfer, and momentum transfer phenomena.

A substantial number of papers have been published on rotary dryers covering various aspects such as drying, residence time distribution, and solids transportation. A static model for counter-current rotary dryer was developed by Myklesstad[1] to obtain a moisture profile for solids in both constant and falling rate periods. Shene et al.[2] developed a mathematical model to predict the solid and drying gas temperature and moisture content axial profiles along a direct contact rotary dryer by focusing on the drying kinetics based on phenomenological models. Shone and Bravo[3] used two different approaches to predict the solid moisture content and solid temperature profiles along a continuous, indirect contact rotary dryer heated with steam tubes by applying heat and mass balances to the solid phase in a differential element of dryer length.

Garcia and Ragazzo[4] proposed a phenomenological mathematical model that describes the continuous drying process. Zabaniotou[5] studied drying of forestry biomass in a rotary dryer to study the influence of air flow rate, temperature, rotation speed, and inclination of a laboratory rotary dryer to biomass residence time and biomass outlet moisture content, and developed a mathematical model for biomass drying. Hatzilyberis et al.[6] measured temperature profiles along the dryer length, the moisture removal, and the solids residence time distribution (RTD) and tested a non-isothermal model under three different regimes of solids flow. Ghoshdastidar et al.[7] developed a numerical heat transfer model in a rotary kiln used for drying and preheating of wet iron ore by including various modes of heat transfer between gas and solids and predicted the length of the kiln as well as axial solid and gas temperature distributions. Krokida et al.[8] obtained drying kinetics data as well as the related thermo-physical properties of olive cake and proposed an appropriate dryer model.

Igauaz et al.[9] developed a model by dividing the dryer into 10 sections and establishing mass and energy balances in each of them to predict air, product moisture, and temperature. Xu and Pang[10] developed a mathematical model to simulate the drying of the woody biomass as chips in a rotary dryer, based on energy, mass balance, and transfer,

experimental drying kinetics of the wood chips, and using literature correlations for the residence time. The model was applied both for co-current and countercurrent rotary dryers.

Ademiluyi et al.[11] studied the effects of inlet air temperatures, inlet air velocities, relative humidities, feed rates, drum drive speeds, and feed drive speeds on heat transfer coefficient and heat load in the material. They also presented models that predict the specific heat transfer coefficient as a function of inlet air temperature and inlet air velocity. Castaño et al.[12] presented a model of a co-current dryer and suggested methods for some improvements in the determination of the drying rate to obtain a more accurate analytical expression.

Sai et al.[13] investigated the residence time distribution (RTD) of solids in a rotary kiln and proposed correlations for mean residence time, hold-up, and dispersion number in terms of operating parameters. They used both an axial dispersion model and tanks-in-series model. Duchesne et al.[14] developed two simple models for solids transportation to understand the underlying phenomena taking place in an industrial rotary dryer. Hatzilyberis and Androutsopoulos[15] carried out RTD studies and correlated mean residence time, space-time, and solids hold-up with the drum operating conditions. Cao and Langrish[16] predicted solids residence time in rotary dryers with three models and compared with both pilot-scale and industrial-scale data.

Renaud et al.[17] developed a complete simulation model for an industrial rotary dryer to account for the heat and mass exchange between the solids and the gas and the variation of the average residence time and model parameters as a function of solids and gas flow rates are presented. Renaud et al.[18] studied the influence of solids feed moisture content on solids mean residence time in a rotary dryer and reported that mean residence time for a moisture content in the range of 8% to 12% is four times higher than for dry solids. They also observed that the moisture content and the drying gas temperature influence significantly the shape of the residence time distribution curve.

Loni and Sai[19] summarized the earlier work in respect to RTD in rotary devices and developed a comprehensive five-parameter model for RTD of solids in a rotary kiln to account for the changing axial velocity and changes in axial dispersion coefficient. Renström[20] developed an industrial method for determining the mean residence time with LiCl as tracer and benchmarked on a laboratory scale against the stop-and-empty method. Thibault et al.[21] experimentally determined that the residence time in a pilot-scale rotary dryer was for four types of solids while varying the solids flow rate, the slope of the dryer, the speed of rotation, and the flow rate of gas. They proposed a correlation to predict the mean residence time for inclined and horizontal rotating dryers and compared with the experimental data. Three models, two based on the product of operating variables and a neural network, are presented and compared.

An analysis of literature indicates that the available information is restricted to modeling of rotary dryers based on fundamental laws of heat transfer and mass transfer, and experimental data is available on rotary drying of food and agricultural products. There is no published information on the study of solids transportation and drying in the same dryer for granular material. However, Chandran et al.[22] used a probability density model for fluidized bed drying using residence distribution function suitable for mixing of solids and drying kinetics. The present study aims to obtain the drying characteristics for non-hygroscopic porous material (sand), and development of population balance model by combining the drying kinetics and residence time distribution function appropriate for the mixing of solids. The present work describes: (i) drying kinetics through batch experiments; (ii) contacting pattern of the dryer through RTD studies; (iii) prediction of continuous dryer performance using RTD and batch kinetics; and (iv) comparison of the predictions on continuous dryer with experimental data.

MATERIALS AND METHODS

The schematic of the experimental set-up is shown in Fig. 1. The experimental set-up consists of a rotating cylinder of 1 meter length with an ID of 122 mm. To drive the cylinder at desired rotational speed, a DC motor was provided. The inclination of the cylinder was varied with the help of a jack mechanism provided at the feed end of the kiln. A vibratory feeder was used to feed the material to the rotary dryer at constant rate. Lifting flights were provided inside the cylinder wall to prevent the slippage of material along the inside surface and to aid in good mixing of the material. Circular dams provided at the exit end with a height of 14 mm and at the entrance end with a height of 19 mm covering, respectively, 20 and 30% of the kiln cross-sectional area. Provisions were made to insert

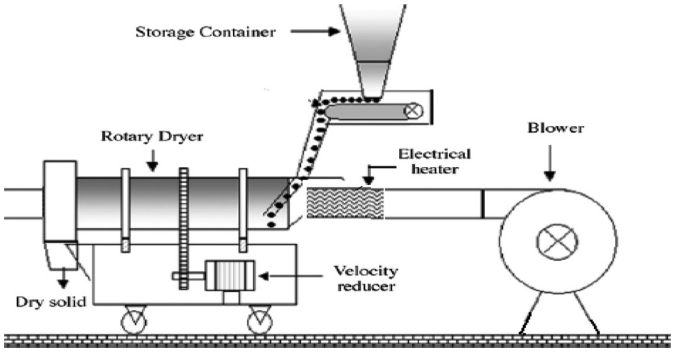

FIG. 1. Schematic of the experimental setup.

thermocouples at the inlet and outlet ends. Air drawn through a blower passes through a heater and the flow rate and temperature of the air were controlled independently by variacs connected to the blower and heater.

The feed (sand) was prepared by adding a known amount of water to a known quantity of solids and mixing the contents thoroughly. The moisture content of the feed was determined by drying a sample of solids in an air oven maintained at 105°C to a constant weight.

Batch Drying

After placing a known amount of the feed material in the dryer, the dryer was provided with a small inclination initially to facilitate the even distribution of the material inside and later was made horizontal. Hot air at known temperature was admitted to the dryer and the progress of the drying was monitored at regular intervals of time by measuring the wet and dry bulb temperatures with digital thermometers. The moisture content of the exit air was calculated using an online humidity calculator and the moisture content of the solids was calculated by material balance. The temperatures at the exit were noted until the drying was complete. The flow rate of the air was measured using anemometer. The experiments were repeated at different operating conditions, as detailed in Table 1.

Residence Time Distribution

Under steady-state conditions, the residence time distribution was determined by introducing the tracer, colored sand, as pulse through the inlet of the cylinder. Samples were collected for a known amount of time at the discharge end of the cylinder at regular intervals of time. The tracer was then separated from the sample manually, and the weight of the tracer and the feed material (non-tracer) were weighed. At the end of the experiment, the feed rate and rotational speed were simultaneously stopped and the material inside the kiln was collected and weighed. This gives the hold-up of the cylinder under those conditions. The range of variables investigated is reported in Table 2. The particle size of the sand used was the same as that used for drying studies. The amount of the tracer used was 25 grams in all the experiments.

TABLE 1
Range of variables studied for drying experiments

Process variable	Range
Particle size, mm	+1 −1.25
Air inlet temperature,°C	52, 65, 75
Initial moisture content of solids, %	3, 4, 5, 8
Air velocity, cm/s	19.5, 23.5, 25.2
Solids feed rate, kg/h	15.72
Rotational speed, rpm	4, 7, 12
Inclination, deg	2.77, 3.47, 4.16

TABLE 2
Range of variables studied for RTD experiments

Process variable	Range
Particle size, mm	+1 −1.25
Solids feed rate, kg/h	10.38, 15.24, 18.48
Rotational speed, rpm	5.5, 10, 15
Inclination, deg	3.00, 3.52, 3.90

Continuous Drying

Initially, hot air at known temperature was admitted into the dryer operating at required rotational speed and inclination until a steady outlet temperature was reached. The wet material was then fed through the vibratory feeder at known rate. After steady state was attained, as indicated by constant wet and dry bulb temperatures at both inlet and outlet, a sample was collected at the exit stream for moisture content determination. The experiments were repeated at different operating conditions, as detailed in Table 1.

RESULTS AND DISCUSSION

Batch Drying

A set of 34 experiments was conducted with 1 kg of material under different operating conditions, viz., air flow rate and its temperature, initial moisture content of solids, and rotational speed of the dryer.

If an amount of M_0 kg of wet solids with moisture content of X_O is charged to a batch dryer through which G kg/min of dry air flows continuously, the fall in moisture content of the solids over a time interval of t_n to t_{n+1} is related to the increase in humidity of the gas over the dryer from the inlet value Y_{GO} to that in the exit Y_{GE}. Then the moisture content of the solids X_{n+1} at t_{n+1} is given by

$$\frac{M_0}{1+X_0}[X_n - X_{n+1}] = G \left[\int_{t_n}^{t_{n+1}} Y_{GE}\, dt - Y_{G0}(t_{n+1} - t_n)\right] \quad (1)$$

The moisture content of the solids in the above equation is expressed as kg of moisture/kg of dry solids. A typical variation in relative moisture content of solids with time is shown in Fig. 2. This curve will be useful directly in determining the time required for drying large batches under the same drying conditions.

A typical variation in rate of drying with initial moisture content is shown in Fig. 3. This curve is much more

TABLE 3
Details of experimental conditions, mean residence time, hold-up, and dispersion number

Run no.	Feed rate, kg/h	Rotational speed, rpm	Inclination, deg	Mean residence time, s	Hold-up, g	Dispersion number, $\times 10^2$
1	10.38	10.0	3.52	185	529	1.370
2	10.38	15.0	3.52	135	376	2.857
3	10.38	15.0	3.90	125	359	2.000
4	10.38	10.0	3.90	177	523	0.833
5	15.24	10.0	3.52	133	549	1.282
6	15.24	15.0	3.90	113	476	2.174
7	15.24	10.0	3.90	165	698	0.806
8	15.24	15.0	3.52	190	795	0.275
9	18.48	5.50	3.00	407	2059	0.310
10	15.24	5.50	3.00	442	1863	0.400
11	18.48	5.50	3.52	335	1701	0.351
12	18.48	5.50	3.90	252	1303	0.439
13	15.24	5.50	3.90	278	1184	0.226
14	15.24	5.50	3.52	315	1337	0.373
15	10.38	5.50	3.00	477	1350	0.231
16	10.38	5.50	3.52	308	850	0.467
17	10.38	5.50	3.90	277	761	0.532
18	10.38	10.0	3.00	266	750	0.287
19	10.38	15.0	3.00	158	478	0.840
20	15.24	10.0	3.00	223	950	0.323
21	15.24	15.0	3.00	175	755	0.457
22	18.48	10.0	3.00	218	1115	0.549
23	18.48	10.0	3.52	183	950	0.592
24	18.48	10.0	3.90	167	845	0.296
25	18.48	15.0	3.00	159	805	0.568
26	18.48	15.0	3.52	129	650	0.769
27	18.48	15.0	3.90	112	555	0.758

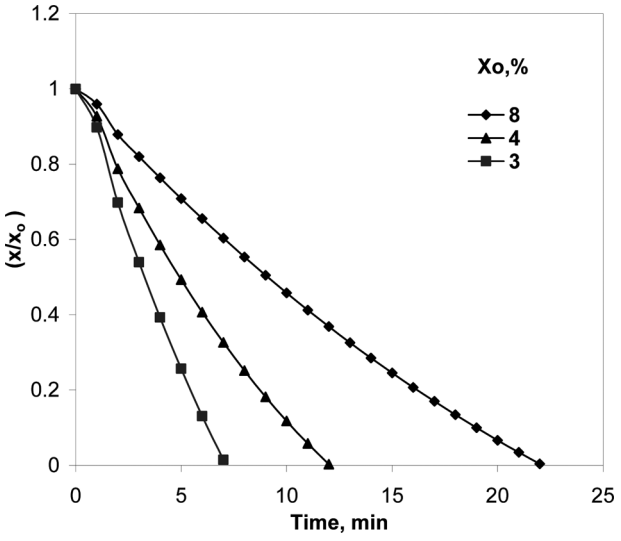

FIG. 2. Variation of relative moisture content of solids with initial moisture content at T = 52°C, V = 25.2 cm/s, N = 12 rpm.

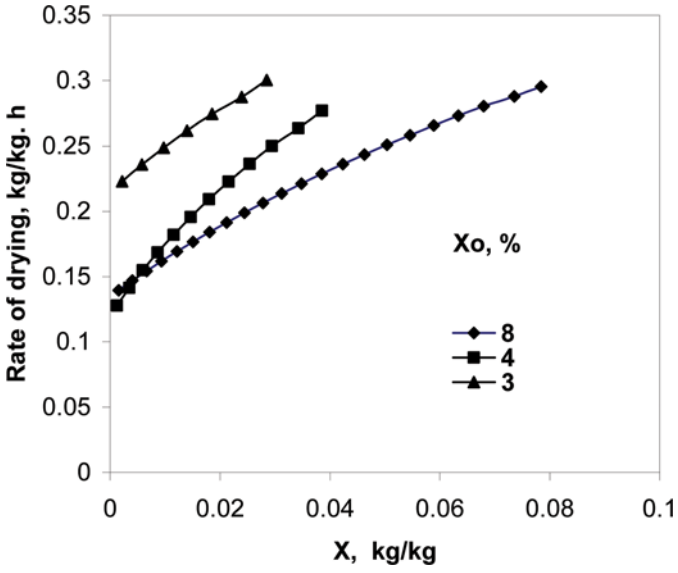

FIG. 3. Variation of drying rate with initial moisture content of solids at T = 52°C, V = 25.2 cm/s, N = 12 rpm (color figure available online).

descriptive of the drying process. Here the total part of the curve constitutes the falling rate period. This is because the initial moisture content of solids is less than the critical moisture content and the drying causes dry spots to appear upon the surface; these spots occupy increasingly larger proportion of the exposed surface as drying proceeds. Since, however, the rate is computed by assuming constant gross surface, the rate must fall even though the rate per unit of wet surface remains constant. This period is called unsaturated surface drying.

Figure 3 illustrates the effect of initial moisture content of the solids on batch drying of solids. An increase in the initial moisture content gives rise to higher (X/X_0) ratio for a given time of drying or decreases the rate of drying at given moisture content of solids. This is because the difficulty of evaporating moisture from the surface will increase with higher initial moisture content and results in decrease of rate of drying. The effect of flow rate of the drying medium on batch drying of solids is shown in Fig. 4. An increase in the flow rate increases the rate of drying at given moisture content of solids. This is because, with increasing air flow rate, the amount of fresh and dry air which evaporates the moisture from the surface increases and hence the rate of drying increases.

The effect of temperature of the heating medium on batch drying of solids is shown in Fig. 5. An increase in the temperature enhances the rate of drying at given moisture content of solids as the driving force for drying increases. The effect of the rotational speed of dryer is shown in Fig. 6. With increase in rotational speed, at given moisture content of solids, the fresh surface comes into contact with dry air more often and hence the rate of drying increases.

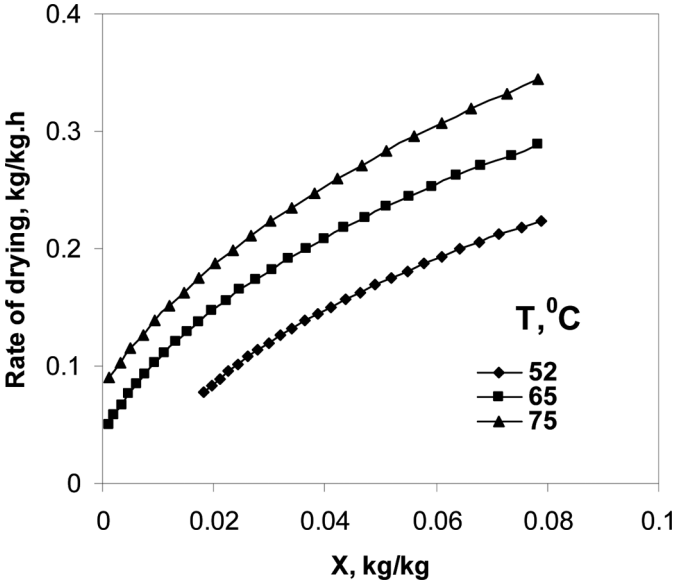

FIG. 5. Variation of drying rate with drying temperature at V = 19.5 cm/s, N = 12 rpm, Xo = 8%.

Residence Time Distribution Studies

A set of 27 experiments was conducted for the purpose of determining the distribution of residence times, the mean residence time of particles, and hold-up of the solids at different operating conditions. A typical tracer output signal is shown in Fig. 7. The RTD seems to consist of a narrow, approximately symmetrical peak. The effect of feed rate of solids, rotational speed, and inclination of the cylinder on RTD is respectively shown in Figs. 7 to 9. It can be noticed that, in general, the mixing increases with increase in feed rate of solids (Fig. 7), which is reflected in the spread of the RTD curves. The other variables, namely the rotational

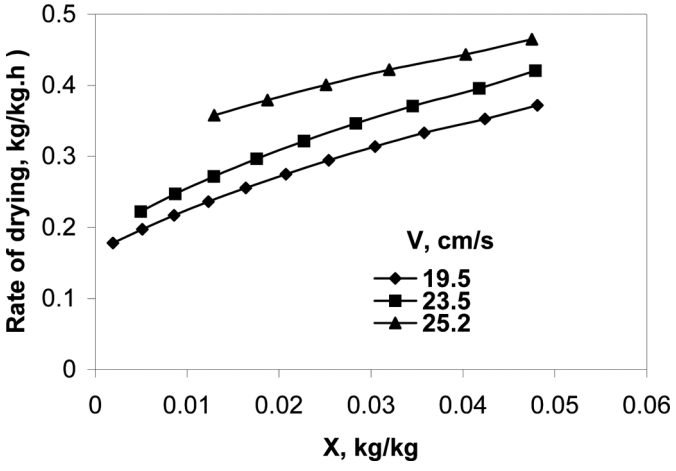

FIG. 4. Variation of drying rate with flow rate of drying medium T = 65°C, N = 12 rpm and X_O = 5%.

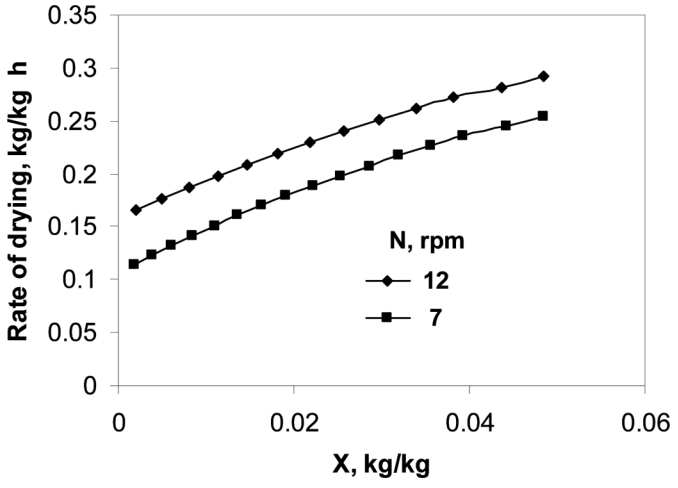

FIG. 6. Variation of drying rate with rotational speed of the dryer at T = 52°C, V = 25.2 cm/s, Xo = 5%.

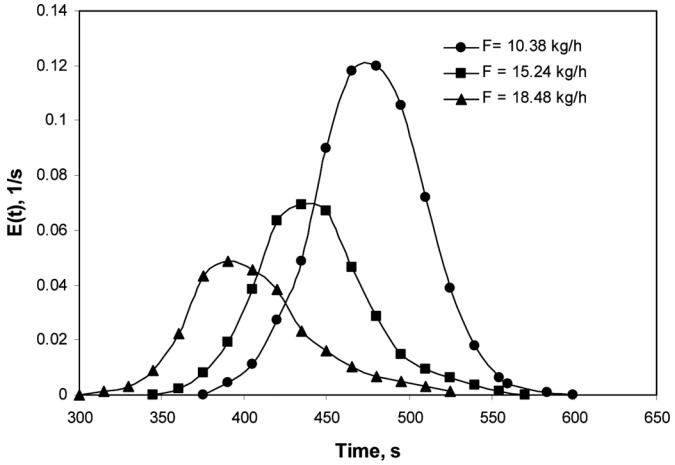

FIG. 7. Effect of feed rate on RTD at N = 5.5 rpm and A = 3.0 deg.

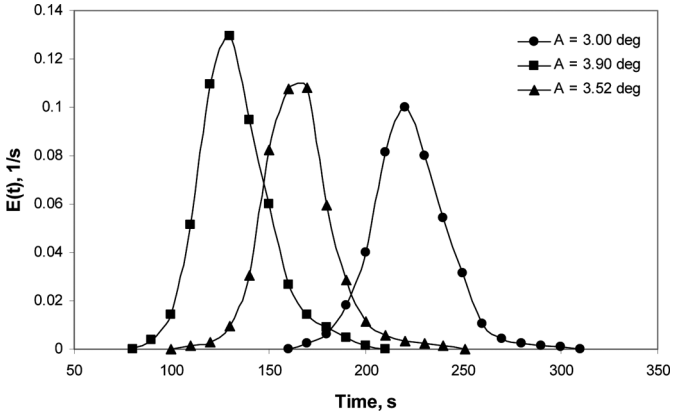

FIG. 9. Effect of angle of inclination on RTD at F = 15.24 kg/h and N = 10 rpm.

speed and inclinations of the cylinder, did not show much change in mixing (Figs. 8 and 9). The time of breakthrough in residence time decreases with increase in either feed rate of solids or rotational speed of the cylinder or inclination of the cylinder. While a decrease in breakthrough time with increase in either rotational speed or inclination of the cylinder is expected, the decrease in breakthrough time with increase in feed rate of the solids is not expected. This is because the mean residence time depends strongly on both rotational speed and inclination of the cylinder compared to the feed rate of solids. However, the decrease in breakthrough time with feed rate of solids is small compared to the other two variables.

The mean residence times calculated from the experimental data using the following equation are reported for all the runs in Table 2.

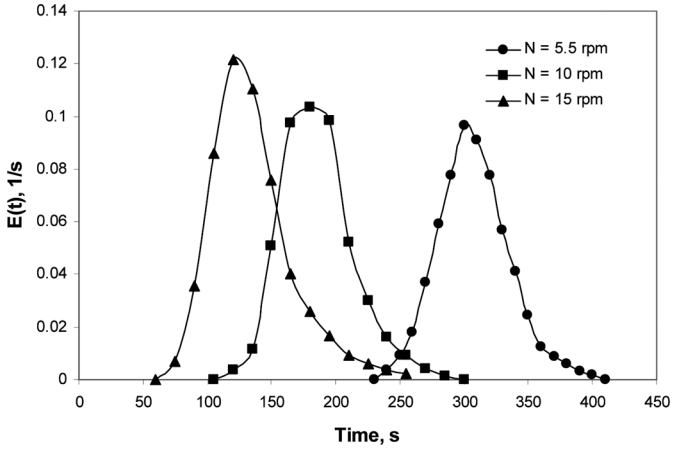

FIG. 8. Effect of rotational speed on RTD at F = 10.38 kg/h and A = 3.52 deg.

$$\tau = \frac{\sum_{i=0}^{\infty} t_i C_i \Delta t_i}{\sum_{i=0}^{\infty} t_i C_i} \tag{2}$$

The mean residence time decreases with increase in either feed rate of solids or rotational speed of the cylinder or inclination of the cylinder. However, the variation in mean residence time with feed rate of solids is small compared to the changes in either rotational speed or inclination of the cylinder. These observations are similar to those reported by Sai et al.[13].The mean residence thus computed is correlated in terms of operating variables by the following equation:

$$\tau = 12200\, F^{-0.11} N^{-0.87} A^{-1.48} \tag{3}$$

Sai et al.,[13] while working on RTD in a rotary kiln with L/D ratio of 40, reported coefficients of −0.072, −0.88, and −1.02 for feed rate, rotational speed, and inclination, respectively. The slight difference in coefficient for inclination in the present study could be due to the small L/D ratio of the present study. In addition, Sai et al.[13] used very low rotational speeds (1 to 3 rpm) compared to the present study. The mean residence time calculated with Eq. (3) is compared with the experimental in Fig. 10.

The variation of hold-up with operating conditions is shown in Table 2. It can be seen from Table 2 that an increase in either angle of inclination or rotational speed of the cylinder results in decrease in hold-up, whereas an increase in feed rate increases hold-up. The variation in hold-up with operating variables is represented by the following correlation.

$$H = 3385\, F^{0.90} N^{-0.86} A^{-1.52} \tag{4}$$

Sai et al.[13] reported coefficients of 0.86, −0.9, and −1.11 for feed rate, rotational speed, and inclination,

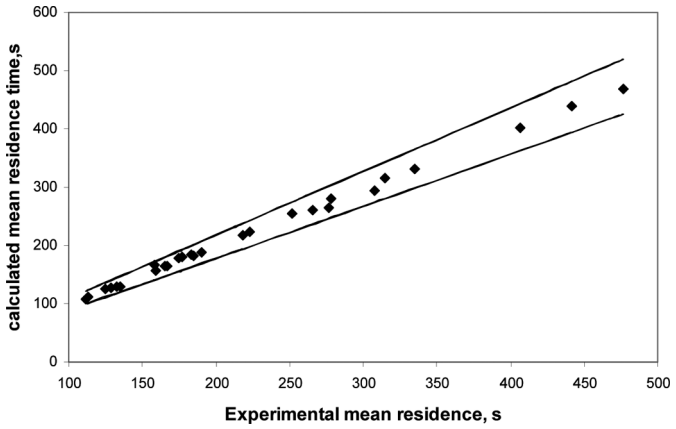

FIG. 10. Comparison of experimental and calculated mean residence times.

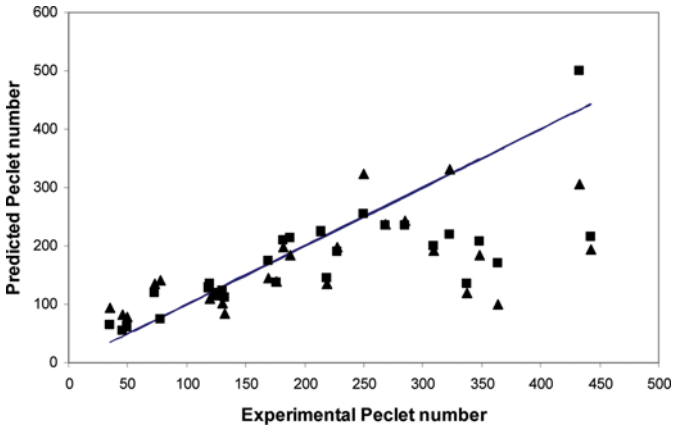

FIG. 12. Comparison of experimental and Peclet numbers (color figure available online).

respectively. As in the case of correlation for mean residence time, the exponent for angle of inclination is different from the present study. The experimental hold-up is compared with that calculated using Eq. (4) in Fig. 11.

The experimental dispersion number calculated by the following equation is listed in Table 2 for various operating conditions:

$$\sigma_\theta^2 = \frac{\sigma^2}{\tau^2} = 2\left(\frac{D}{uL}\right) \tag{5}$$

Where

$$\sigma^2 = \frac{\sum_{i=0}^{\infty} t_i^2 C_i \Delta t_i}{\sum_{i=0}^{\infty} t_i C_i} - \tau^2 \tag{6}$$

The dispersion number, which gives a measure of the extent of longitudinal back mixing, is calculated using axial dispersion model as follows: assume a dispersion number and calculate E(t) from the model. The standard deviation between this vale and experimental E(t) values was found. The dispersion number, which minimizes the standard deviation between the experimental values and calculated values, is obtained. The dispersion number is correlated in terms of process variables by the following correlation:

$$\frac{D}{uL} = \frac{1}{Pe} = 0.000121\, F^{-0.13}\, N^{-0.86}\, A^{1.94} \tag{7}$$

The Peclet number calculated from the above equation is compared with the experimental in Fig. 12. The residence time distribution function obtained with the dispersion number is compared with the experimental in Figs. 13 and 14.

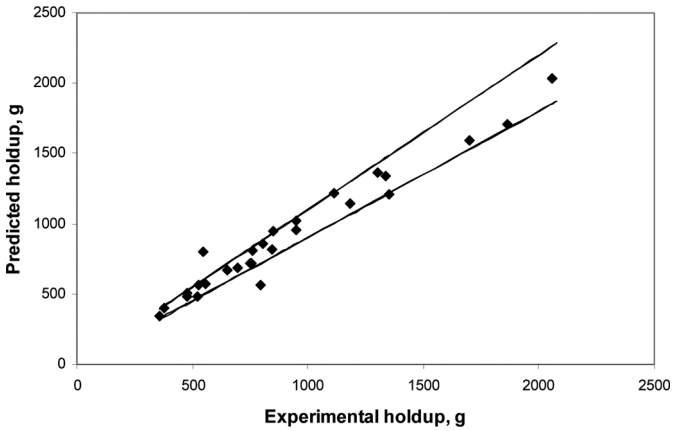

FIG. 11. Comparison of experimental and calculated holdup of solids.

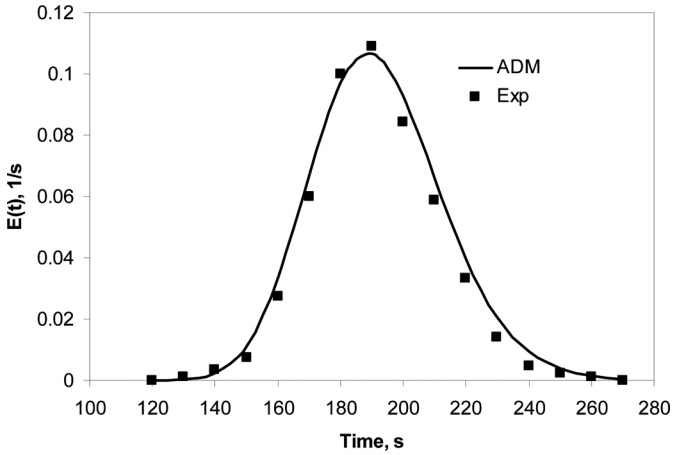

FIG. 13. Comparison of predicted RTD using ADM with experimental RTD at F = 15.24 kg/h, N = 15 rpm and A = 3.52 deg.

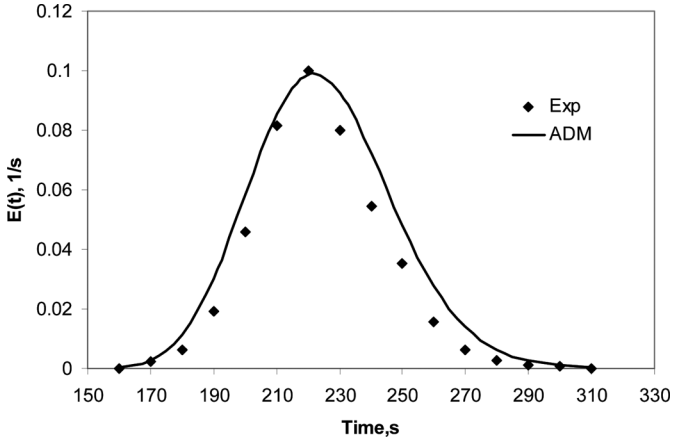

FIG. 14. Comparison of predicted RTD using ADM with experimental RTD at F = 15.24 kg/h, N = 10 rpm and A = 3.0 deg.

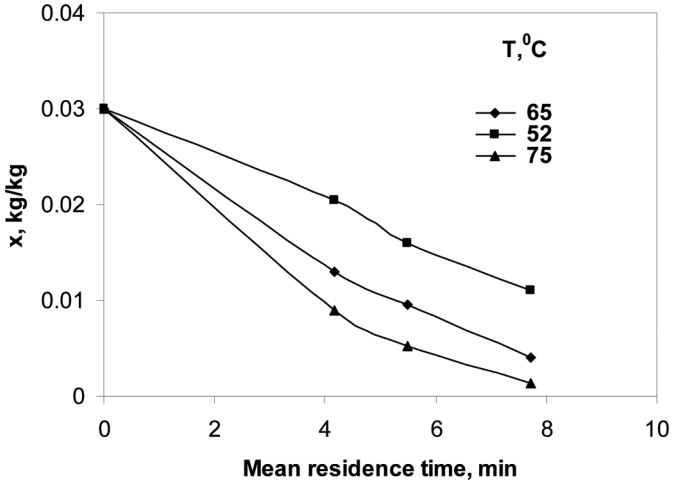

FIG. 16. Effect of temperature of the heating medium on average moisture content of the solids in the exit stream at V = 19.5 m/s, N = 12 rpm, X_O = 3%.

Continuous Drying of Solids

A set of 24 experiments was conducted covering the range as detailed in Table 1. Figure 15 shows the effect of the rotational speed of the dryer on average moisture content of the solids in the exit stream with mean residence time of solids, wherein it can be seen that an increase in rotational speed reduces the average moisture content (or enhances the rate of drying of solids). This observation is similar to that obtained in batch drying. An increase in rotational speed increases the showering action of the solids, leading to better contact between the solids particles with the drying medium. This leads to moisture content in the solids exiting the dryer even though the residence time decreases with increase in rotational speed.

Figure 16 shows the effect of temperature of the heating medium on average moisture content of the solids exiting from the dryer. Each point corresponds to a mean holding time. It can be seen from the figure that an increase in temperature reduces the average moisture content of the solids in the exit stream (or enhances the drying rate of the solids). With increase in temperature of the drying medium, the amount of heat supplied to the surface increases and hence the rate of drying increases.

Figure 17 shows the effect of air flow rate on average moisture content of the solids in the exit stream wherein it can be seen that an increase in the air flow rate reduces the average moisture content (or enhances the rate of drying of solids). This observation is also similar to that obtained in batch drying. With increase in air flow rate, the amount of fresh and dry air which evaporates the moisture from the surface increases and hence the rate of drying increases.

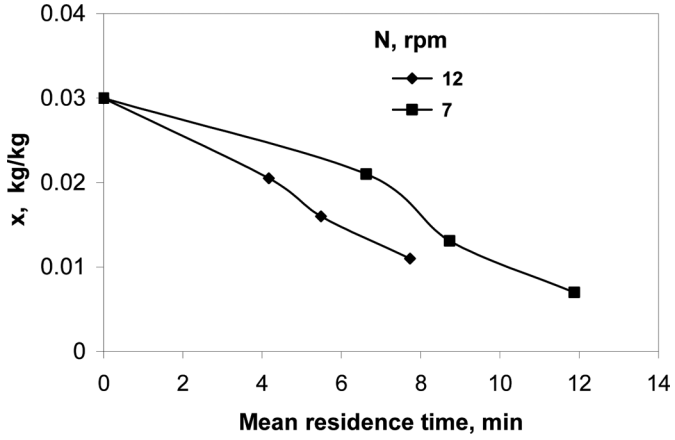

FIG. 15. Effect of rotational speed of the dryer on average moisture content of the solids in the exit stream at T = 52°C, V = 19.5 cm/s, X_0 = 3%.

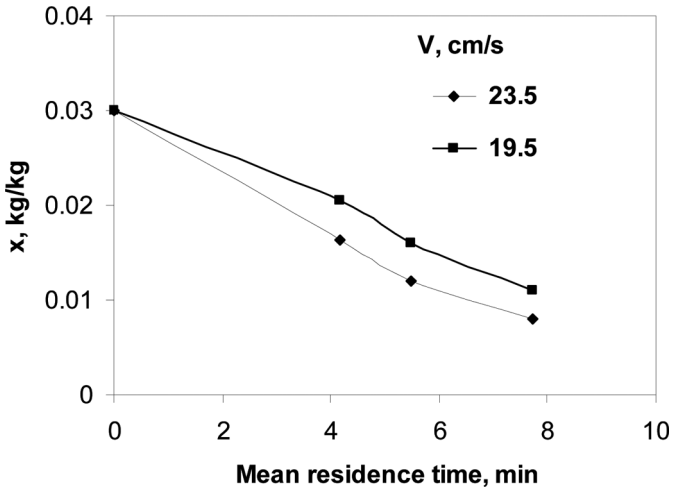

FIG. 17. Effect of air flow rate on average moisture content of the solids in exit stream at T = 52°C, N = 12 rpm, X_O = 3%.

Comparison of the Average Moisture Content of the Solids in the Exit Stream of the Continuous Dryer with That Predicted Using the Batch Data and Axial Dispersion Model

The variation of drying process with operating variables, viz., initial moisture content of solids, flow rate, and temperature of the heating medium, rotational speed of the dryer is similar both in batch and continuous drying. Thus the experimental data from batch drying is used to make predictions using an axial dispersion model for the average moisture content of the solids in the continuous mode.

The average moisture content of solids in the exit stream from axial dispersion model is given by

$$\overline{X} = \int_0^\infty [X(t)_b E(t)\, dt] \tag{8}$$

Where E (t) is given by[23]

$$C(\theta) = \left\{ \begin{array}{l} \frac{1}{4}\left(\frac{Pe}{\pi}\right)^{1/2}\frac{(\theta+1)}{\theta^{3/2}} - \left(\frac{1}{Pe\pi}\right)^{1/2}\left(\frac{\theta^{1/2}}{(\theta+1)}\right) \\ \left[\psi\left(\frac{\theta}{\theta+1}\right)\left\{\frac{1}{2\theta} - \frac{1}{\theta+1} + \frac{Pe(1-\theta)^2}{4\theta^2}\right\}\right] \\ + \frac{1}{(1+\theta)^2}\chi\left(\frac{\theta}{\theta+1}\right) \end{array} \right\} \exp\left[-\frac{Pe(1-\theta)^2}{4\theta}\right] \tag{9}$$

Where

$$\psi(\zeta) = \sum_{k=0}^{\infty}(-1)^k\left[\frac{2\zeta(1-\zeta)}{Pe}\right]^k \phi_k(\zeta)$$

with

$$\phi_k(\zeta) = 1.3.5\ldots(2k+1)\left[\frac{1}{(2k+1)} - 6\zeta + 4(k+1)\zeta^2\right]$$

and

$$\chi(\zeta) = \sum_{k=0}^{\infty}(-1)^k \left\{ \begin{array}{l} k\left[\frac{2\zeta(1-\zeta)}{Pe}\right]^{(k-1)}\frac{2(1-2\zeta)}{Pe}\phi_k(\zeta) \\ + \left[\frac{2\zeta(1-\zeta)}{Pe}\right]^k \Omega_k(\zeta) \end{array} \right\}$$

with

$$\Omega_k(\zeta) = 1.3.5\ldots(2k+1)[-6 + 8(k+1)\zeta]$$

The above equation is an approximate form of the exact solution to the axial dispersion model for an impulse input. The axial convective velocity and the axial dispersion coefficient are uniquely represented by the dimensionless Peclet number (Pe). Even though multi-parameter models[13,19] are reported, this single parameter model was selected because of its simplicity. The Peclet number necessary to use in Eq. (9) is evaluated with Eq. (7).

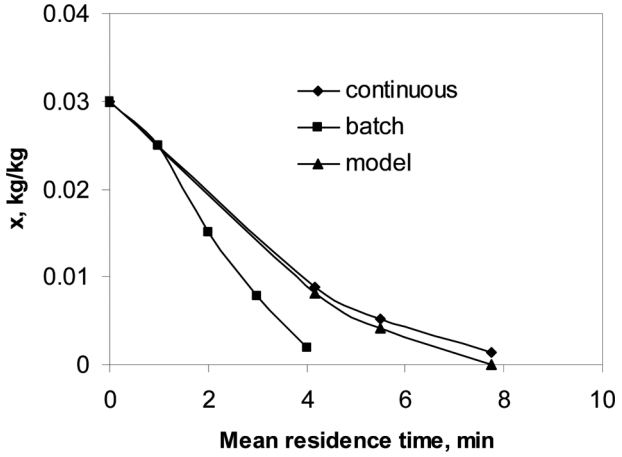

FIG. 18. Comparison of experimental and predicted average moisture content of solids in the exit stream at T = 75°C, V = 19.5 cm/s, X_O = 3%, %, N = 12 rpm, F = 15.72 kg/h.

The average moisture content of solids in the exit stream calculated using the above equations is compared satisfactorily with experiments in Figs. 18 and 19 at two different sets of conditions.

The variation of average moisture content of solids with clock time in batch drying under the same set of conditions (rotational speed, air flow rate, inlet air temperature, and initial moisture content) as continuous drying is also shown in Figs. 18 and 19. The batch dryer was horizontal and continuous dryer was inclined. It is seen from the figures that the batch drying gives lower moisture content for the solids compared to that of a continuous drying for a given residence time of solids. This is because of lesser hold-up of solids under batch conditions and hence the bed height would be less and the exposed area for drying would be less. The deviation is more at higher residence times.

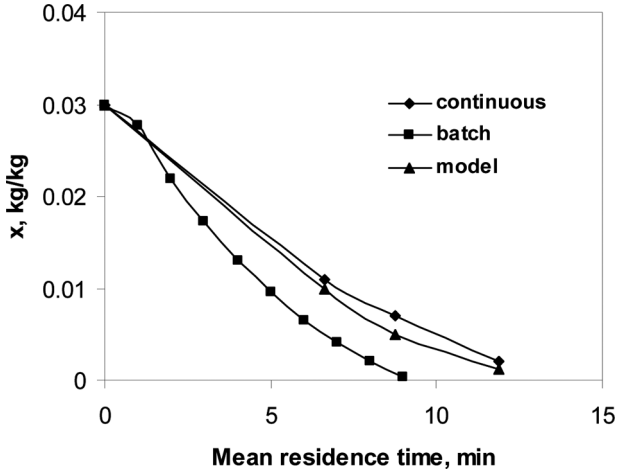

FIG. 19. Comparison of experimental and predicted average moisture content of solids in the exit stream at T = 65°C, V = 19.5 cm/s, X_O = 3%, %, N = 7 rpm, F = 15.72 kg/h.

CONCLUSIONS

Batch-drying experiments were conducted in a horizontal rotary dryer for obtaining kinetics at different operating conditions, viz., inlet air temperature, flow rate of the air, rotational speed of the dryer, and inlet moisture content of the solids. It is observed that as the inlet air temperature or flow rate of the air or the rotational speed of the dryer increases, the rate of drying increases. Among the above three variables, the effect of inlet air temperature is more predominant. In addition, an increase in the initial moisture content of solids gives rise to higher moisture content in the solids for a given time of drying.

It is observed from the experimental data of the present study on co-current drying of solids that the effect of variables such as temperature and flow rate of the heating medium and rotational speed of the dryer on drying rate is qualitatively similar to that reported earlier for batch drying of solids. An increase in the mean holding time reduces the average moisture content of the solids in exit stream.

Assuming axial mixing of solids within the rotary dryer, the performance of the continuous dryer was predicted based on batch drying rate curve and was found to compare satisfactorily with that of the experimental data obtained on the continuous dryer.

NOMENCLATURE

A	angle of inclination of dryer, deg
C	concentration of tracer, kg/s
E (t)	residence time distribution of solids, 1/min,
F	mass flow rate of the solids, kg/h
G	mass flow rate of the air, kg/min
H	hold-up of the cylinder, g
M_O	amount of solids placed in batch rotary dryer, kg
N	rotational speed of the dryer, rpm
Pe	Peclet number
T	temperature,°C
t	time, min
t_m	mean residence time, min
V	air velocity, m/s
X_O	initial moisture content of the solids, kg of moisture/kg of dry solids
X_n	moisture content of the solids at time t_n, kg of moisture/kg of dry solids
Y_{GO}	humidity of the gas at the outlet at time $t = 0$, kg of moisture/kg of dry air
Y_{GE}	humidity of the gas at the outlet at time t, kg of moisture /kg of dry air
θ	dimensionless time, t/t_m
σ^2	variance of data points, $1/s^2$
σ_θ^2	dimensionless variance

ACKNOWLEDGMENTS

The author wishes to acknowledge the support of Mr. M. Narasimhulu and Mr. Avaneendra Linga in carrying out the experiments.

REFERENCES

1. Mykelstad, O. Heat and mass transfer in rotary dryers. *Chem. Eng. Progr.* **1963**, *59*, 129–137.
2. Shene, C.; Cuhillos, F.; Perez, R.; Alvarez, P.I. Modelling and simulation of a direct contact rotary dryer. *Drying Technology* **1996**, *14*(10), 2419–2433.
3. Shone, C.; Bravo, S. Mathematical modelling of indirect contact rotary dryers. *Drying Technology* **1998**, *16*(8), 1567–1583.
4. Gracia, M.A.; Ragazzo, A. Mathematical modeling of continuous dryers using a mass transfer properties and product–air equilibrium relation. *Drying Technology* **2000**, *18*, 67–75.
5. Zabaniotou, A.A. Simulation of forestry biomass drying in a rotary dryer. *Drying Technology* **2000**, *18*(7), 1415–1431.
6. Hatzilyberis, K.S.; Androutsopoulos, A.P.; Salmas, C.E. Indirect thermal drying of lignite: Design aspects of a rotary dryer. *Drying Technology* **2000**, *18*(9), 2009–2049.
7. Ghoshdastidar, P.S.; Bhargava, G.; Chhabra, R.P. Computer simulation of heat transfer during drying and preheating of wet iron ore in a rotary kiln. *Drying Technology* **2002**, *20*(1), 19–35.
8. Krokida, M.K.; Maroulis, Z.B.; Kremalis, C. Process design of rotary dryers for olive cake. *Drying Technology* **2002**, *20*(4&5), 771–788.
9. Iguaz, A.; Esnoz, A.; Martinez, M.; Lopez, A.; Vırseda, P. Mathematical modelling and simulation for the drying process of vegetable wholesale by-products in a rotary dryer. *J. Food Eng.* **2003**, *59*, 151–160.
10. Xu, Q.; Pang, S. Mathematical modeling of rotary drying of woody biomass. *Drying Technology* **2008**, *26*, 1344–1350.
11. Ademiluyi, F.T.; Abowei, M.F.N.; Puyate, Y.T.; Achinewhu, S.C. Effects of drying parameters on heat transfer during drying of fermented ground cassava in a rotary dryer. *Drying Technology* **2010**, *28*, 550–561.
12. Castano, F.; Rubio, F.R.; Ortega, M.G. Modeling of a co-current rotary dryer. *Drying Technology* **2012**, *30*, 839–849.
13. Sai, P.S.T.; Surender, G.D.; Damodaran, A.D.; Suresh, V.; Philp, Z.G.; Sankaran, V. Residence time distribution and material flow studies in rotary kiln. *Met. Trans.* **1990**, *21B*, 1005–1011.
14. Duchesne, C.; Thibault, J.; Bazin, C. Modeling of the solids transportation within an industrial rotary dryer: A simple model. *Ind. Eng. Chem. Res.* **1996**, *35*, 2334–2341.
15. Hatzilyberis, K.S.; Androutsopoulos, G.P. An RTD study for the flow of lignite particles through a pilot rotary dryer. Part I: Bare drum case. *Drying Technology* **1999**, *l7*(4&5), 745–757.
16. Cao, W.F.; and Langrish, T.A.G. Comparison of residence time models for cascading rotary dryers. *Drying Technology* **1999**, *17*(4&5), 825–836.
17. Renaud, M.; Thihault, J.; Trusiak, A. Solids transportation model of an industrial rotary dryer. *Drying Technology* **2000**, *18*(4&5), 843–865.